



A Novel Method for the Synthesis of Sr₂CeO₄ Blue Nano-Phosphor and Its Characterization

Fahd Al-Wadaani

Taibah University, College of Science, Chemistry Department, Almadinah 30002 Saudia Arabia.

Received 20 Jul 2017
Revised 25 Dec 2017
Accepted 29 Dec 2017

Keywords

- ✓ Sr₂CeO₄,
- ✓ Blue phosphor,
- ✓ Nanoparticles,
- ✓ Cerate.

Fwadaani@taibahu.edu.sa ;
Phone: +966 55 556 6049
Fax:

Abstract

Nanoparticles of the blue phosphor Sr₂CeO₄ were synthesized using a novel method. An oxido reduction took place between a mixture of nitrate salts of strontium and cerium with oxalic acid giving place to the formation of a precursor that will be heat treated at 850 °C to lead to the formation of the desired strontium cerate. The precursor was characterized by differential scanning calorimetry (DSC), The as prepared blue phosphor powder was characterized by X-ray diffraction (XRD), Brunauer–Emmett–Teller technique (BET), transmission electron microscopy (TEM), scanning electron microscopy (SEM), energy dispersive spectroscopy (EDS), and its luminescent properties were investigated. The nanosized nature of the particles was confirmed. The nano-phosphor exhibits an intense blue emission at 466 nm when excited with a 325 nm radiation.

1. Introduction

Oxide-based photoluminescent materials activated by rare-earth ions are implicated in lighting, solar cells, optical applications and field emission displays (FEDs). The syntheses of stable and efficiently luminescent materials which emit in the blue region are of particular interest. Consequently, Sr₂CeO₄, which has orthorhombic symmetry and exhibits blue luminescence as a result of charge transfer (CT) transitions has received growing attention since its discovery through combinatorial chemistry by Danielson et al in 1998 [1].

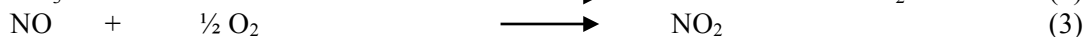
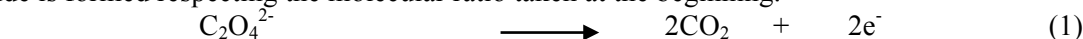
In addition to the combinatorial method, there are numerous established methods for the preparation of Sr₂CeO₄, including solid-state reaction, sol–gel, microwave-assisted solvothermal, sol–gel auto combustion, co-precipitation method and pulsed laser deposition [1-4]. For instance, a comparison of Sr₂CeO₄ blue phosphors prepared via two methods; a solid-state reaction and a microwave-assisted solvothermal process showed that a desirable particle size and enhanced luminescence properties are obtained via the latter method [3]. Similarly, it has been reported that the synthesis of Sr₂CeO₄ via the sol–gel PVA route produces higher luminescence intensity than the solid state reaction method [5]. Additionally, Sr₂CeO₄ prepared from the heat treatment of Ce(III)-doped strontium oxalate shows photoluminescence emission. However, this method also produced some undesirable phases, such as SrCeO₃ and SrCO₃ [6]. Ferrari et al observed that 25 mol% cerium-doped strontium oxalate contained the optimal composition for preparing Sr₂CeO₄ blue phosphors with desirable luminescent property [7]. However, even at this optimal composition the SrCeO₃ and SrCO₃ and phases were still detected [7]. Moreover, nanocrystalline Sr₂CeO₄ thin films grown on silicon substrates by laser ablation show the same photoluminescence as that of powder samples [4]. The presence of unwanted species such as SrCO₃, CeO₂ and SrCeO₃ has been an enduring problem in the synthesis of Sr₂CeO₄. Thus, the development of efficient and inexpensive methods for the preparation of pure Sr₂CeO₄ remains a challenge.

In the present study, pure Sr₂CeO₄ nanoparticles were prepared via the thermal decomposition of an oxalate precursor prepared in the solid state using a new method [8-13]. The resulting powder was characterized by X-ray powder diffraction (XRD), scanning electron microscopy (SEM), energy dispersive spectroscopy (EDS), transmission electron microscopy (TEM), fluorescence spectroscopy and the BET method.

2. Materials and Methods

2.1. Synthesis of the strontium cerate Sr_2CeO_4

The strontium cerate was prepared as follows. A well ground mixture of strontium nitrate tetrahydrate $Sr(NO_3)_2 \cdot 4H_2O$, cerium (III) nitrate hexahydrate $Ce(NO_3)_3 \cdot 6H_2O$ and oxalic acid dihydrate $H_2C_2O_4 \cdot 2H_2O$ in the molar ratio 2/1/8 respectively, was heated on a hotplate at $160^\circ C$. An evolved orange red gas is observed when heating. The reduction of the nitrate anions by the oxalate leads to the formation of NO gas (Equations 1 and 2) which is oxidized in air to give NO_2 (Equation 3). The strontium and cerium cations are then complexed to the oxalic acid [8-13]. Monometallic or bimetallic complexes can be formed. The most important fact is that the two metals are intimately mixed and when the formed oxalate precursor is decomposed at higher temperature, a mixed oxide is formed respecting the molecular ratio taken at the beginning.



The precursor was thermally decomposed at $850^\circ C$, for 2 hours, in a tubular furnace open both sides. The strontium cerate formation starts at $800^\circ C$ and at $1200^\circ C$ its thermal decomposition is observed[14].

2.2. Characterization

In order to verify the crystallographic purity of the prepared samples a Shimadzu X-ray diffractometer 6000 equipped with a Ni filter and a Cu-K α radiation (1.5406 \AA) source was used. The adsorption-desorption isotherms of liquid nitrogen on the phosphor nanoparticles were obtained using a Micromeritics ASAP 2020 surface area and porosity analyzer. The morphology, shape and size of the particles in the powder were investigated by observation with a Jeol JEM – 1400 Flash transmission electron microscope operated at 120 kV and a FEI Quanta FEG 250 scanning electron microscope. Finally the photoluminescence of the well characterized Sr_2CeO_4 nanophosphor was studied on a Shimadzu RF-5301PC spectrofluorometer.

3. Results and discussion

3.1. Characterization of the as prepared strontium cerate

3.1.1. X-ray diffraction XRD

X-ray diffraction permits to identify the crystallized phase existing in the powder. Figure 1 depicts the XRD pattern of the obtained powder. All the peaks were indexed in accordance with the J.C.P.D.S. file # 89-5546 corresponding to the orthorhombic phase of the strontium cerate Sr_2CeO_4 with cell parameters $a=6.117 \text{ \AA}$, $b=10.346 \text{ \AA}$ and $c=3.597 \text{ \AA}$.

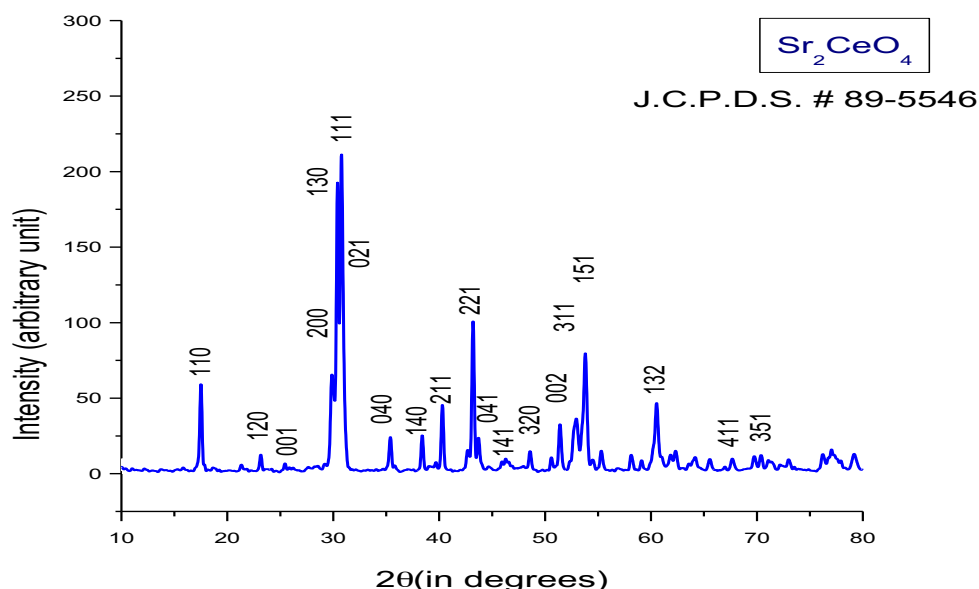


Figure 1: XRD pattern of the as prepared Sr_2CeO_4 nanophosphor prepared at $850^\circ C$

A structure where both strontium and cerium are in an octahedral environment surrounded each one by six oxygen atoms. A particles size estimation D_{xrd} could be obtained by using the Scherrer formula $D_{xrd} = 0.9 \lambda / B \cdot \cos\theta$, where λ is the wavelength, in this case $\lambda = 1.5406 \text{ \AA}$, B is the full width at half maximum (FWHM) and θ

is the Bragg angle. Actually it is difficult to use this formula when peaks are superposed in the pattern, so calculation was done on the isolated (110) diffraction peak. It was found a particles size of 43.8 nm.

3.1.2. BET Brunauer Emmet Teller technique isotherms

The adsorption desorption curves are presented in Figure 2. These curves are classified as type IV. An hysteresis between adsorption and desorption curves is observed indicating the presence of mesopores. It is a B type hysteresis suggesting presence of pores with slits shape. The resulting calculation of the specific surface area with the BET method gives a value of $3.5 \text{ m}^2/\text{g}$ a relatively small value than expected. An estimation of the particles size was done using the formula $D_{\text{BET}} = 6000/S.d$ where S is the specific surface area and d is the density. The value of the calculated D_{BET} was found to be of 310 nm. It is expected now that the particles are very agglomerated. Thus the agglomeration of the particles reduces the surface available for the nitrogen N_2 adsorption. Indeed calculation leads to higher particles size.

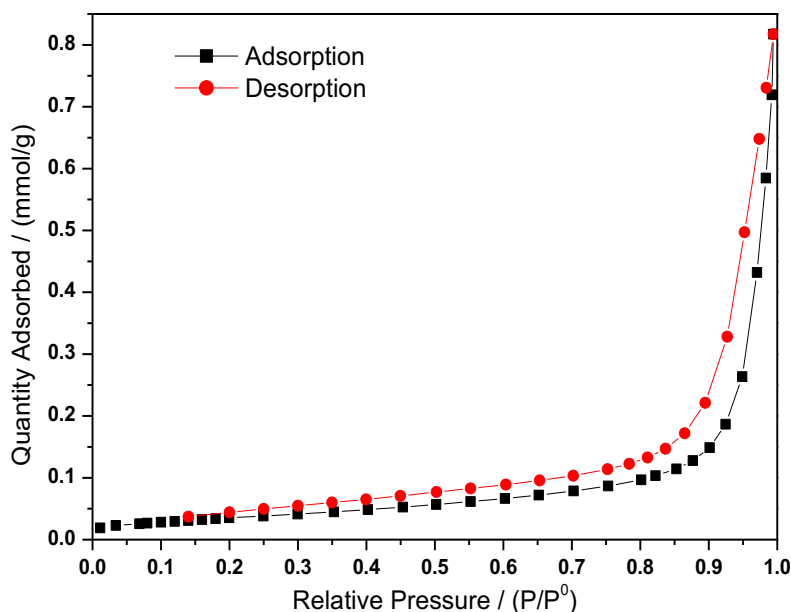


Figure 2: BET adsorption desorption curves of Sr_2CeO_4 nanophosphor prepared at 850°C

3.1.3. Scanning Electron microscopy SEM and EDS

The observation of the powder in the SEM gives a good explanation to the high D_{BET} value. The particles are highly agglomerated (Figure 3a and 3b). The agglomerates are of 1 to 5 microns in size. Separated particles could not be observed even at higher magnification. The agglomerates have a parallelepiped shape as if the powder is being assembled to form bigger crystallites. On the other hand, the EDS spectrum shown in Figure 4, the composition of the prepared strontium cerate was confirmed. The presence of the carbon peak is due to the tape used for sample deposition that contains a conductive carbon to avoid the charge accumulation on the sample. As it can be seen all the elements are present in the ratio 2/1/4 for Sr/Ce/O respectively.

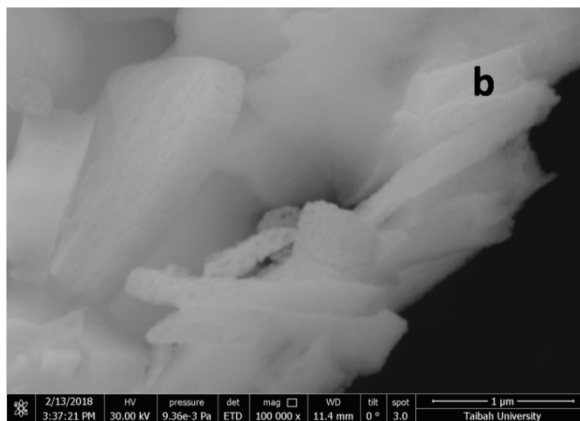
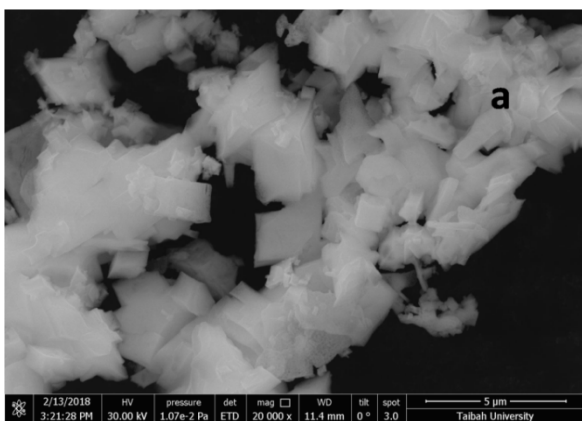


Figure 3: SEM micrographs of Sr_2CeO_4 nanophosphor observed at (a) x30000 and (b) x60000

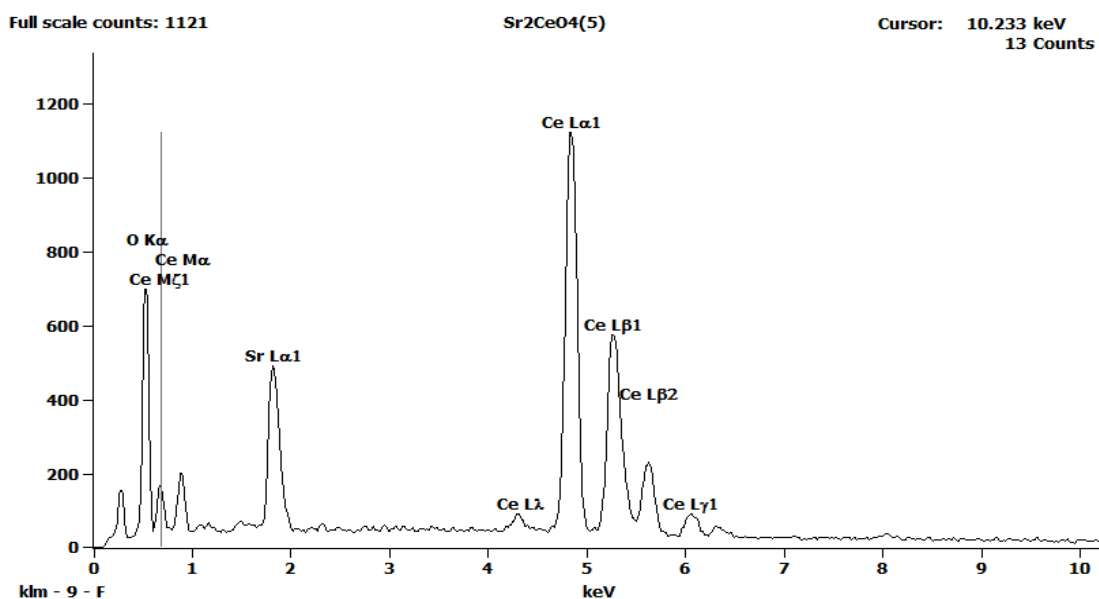


Figure 4 : EDS spectrum of Sr_2CeO_4 nanophosphor prepared at 850°C observed in SEM

3.1.4. Transmission electron microscopy TEM

The micrographs obtained from the transmission electron microscope observation are given in Figures 5a and 5b corresponding to magnifications at x300000 and x500000 respectively. It has to be noted that the sample, when prepared to the observation in transmission microscope, was well ground and then sonicated for 15 minutes. This helps to break the agglomeration and obtain fractions of the agglomerates. The particles that were agglomerated are now well defined in shape and size. The particles seem to offer still slits shape for the pores if assembled again (Figure 5a). They are stacked parallel to each other. At higher magnification the size of the nanoparticles was found to be around 10 nm with distinguished shape of hexagonal nanoplates.

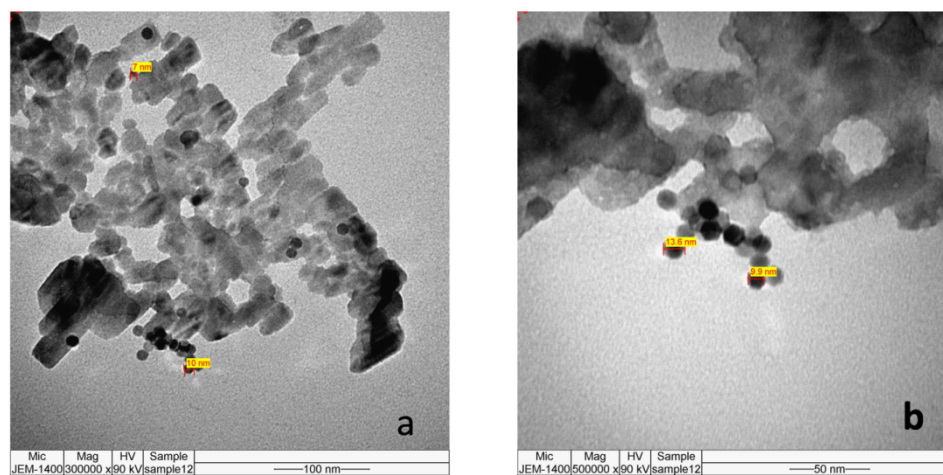


Figure 5: TEM micrographs of Sr_2CeO_4 nanophosphor observed at (a) x300000 and (b) x500000

3.2. Photoluminescence of the as prepared Sr_2CeO_4 nanophosphor

When the Sr_2CeO_4 phosphor is excited under 325 nm, an emission occurs with an intense peak located in the blue region of the spectrum at 466 nm. This result was in accordance with papers published earlier [14-15]. However, what was seen earlier is only one large band enveloping both of the two bands at 372 nm and 466 nm. It is believed that if the emission intensity was higher, then the two bands will overlap and a large band will be observed. It is worthy to note that the emission is due to the charge transfer between ligand O^{2-} and metal Ce^{4+} . More papers were published recently dealing with the use of this material as white phosphor when doped adequately [16-19].

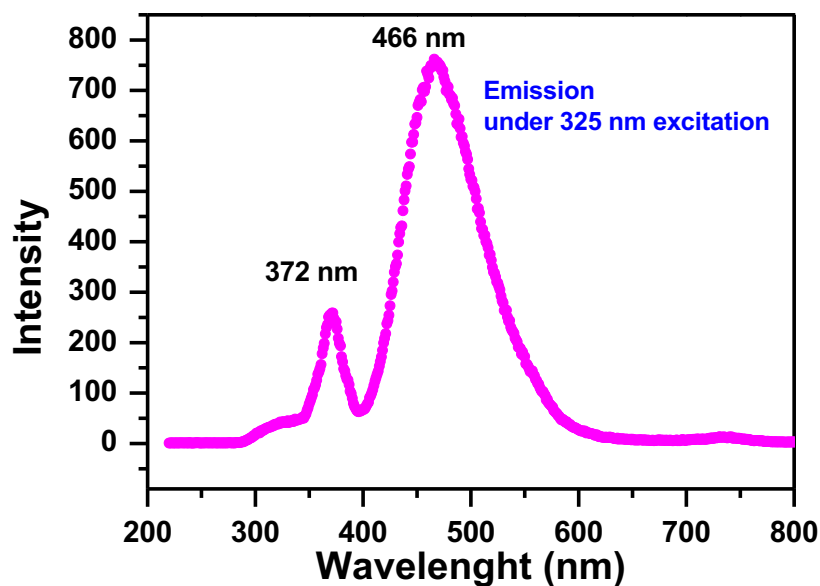


Figure 6: Emission spectrum of Sr_2CeO_4 nanophosphor under excitation with 325 nm radiation.

The CIE diagram (Commission Internationale de l'Éclairage) is given in Figure 7. The calculated (x; y) chromaticity coordinates were found to be of (0.15; 0.19) that are located in the blue region of the diagram.

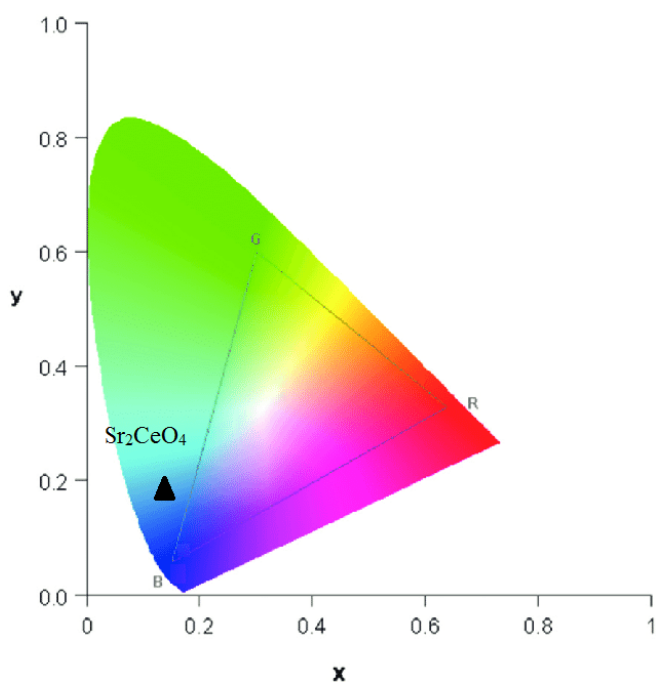


Figure 7: Plot of colour coordinates in the CIE 1931 chromaticity diagram for Sr_2CeO_4 phosphor

Conclusion

Nanoparticles of the blue phosphor Sr_2CeO_4 were successfully synthesized using a new process. The synthesis undergoes in the solid state between oxalic acid and nitrate salts of the strontium and cerium. A precursor was obtained and decomposed at 850 °C. The characterization of the obtained powder shown that the nanoparticles were highly agglomerated. A blue emission was observed when the phosphor was excited under 325 nm radiation. The coordinates of its chromaticity were found of (0.15; 0.19) located in the blue region of the diagram.

References

1. E. Danielson, M. Devenney, D.M. Giaquinta, J.H. Golden, R.C. Haushalter, E.W. McFarland, D.M. Poojary, C.M. Reaves, W.H. Weinberg, X.D Wu, *J. Mol. Struct.*, 470 (1998) 229–235.
2. M. Stefanski, L. Marciniak, D. Hreniak, W. Strek, *Mater. Res. Bull.*, 76 (2016) 133–139.
3. C. Lu, T. Wu, C. Hsu, *J. Lumin.*, 130 (2010) 737–742.
4. N. Perea, G.A. Hirata, *Opt. Mater.* 27 (2005) 1212–1216.
5. R. Seema, K. Nandakumar, *J. Lumin.* 131 (2011) 2181–2184.
6. L.A. Rocha, M.A. Schiavon, C.S. Nascimento Jr., L. Guimarães M.S. Góes, A.M. Pires C.O. Paiva-Santos, O.A. Serra, M.A. Cebim, M.R. Davolos, J.L. Ferrari, *J. Alloy. Compd.* 608 (2014) 73–78.
7. J.L. Ferrari, A.M. Pires, O.A. Serra, M.R. Davolos, *J. Lumin.* 131 (2011) 25–29.
8. H. Yang, S. Seo, M. Abboudi and P. H. Holloway, *J. Ceram. Process. Res.*, 8 (2007) 256-260.
9. N. Kadiri, A. Ben Ali, M. Abboudi and E. Moran, *Phys. Chem. News* 44 (2008) 11-14.
10. M. Messali, F. Al Wadaani, H. Oudghiri-Hassani, S. Rakass, S. Al Amri, M. Benaissa, M. Abboudi *Mater. Let.* 128 (2014) 187–190.
11. H. Oudghiri-Hassani, S. Rakass, F. Al Wadaani, K. J. Al-ghamdi, A. Omer, M. Messali, M. Abboudi, *J. Taibah Univ. Sci.*, 9 (2015) 508-512.
12. R. Al Hazmi, H. Oudghiri-Hassani, F. Al Wadaani and M. Abboudi, *Mor. J. Chem.* 4 (2016) 324-331.
13. C. H. Lu, T. Y. Wu and C. H. Hsu, *J. Lumin.* (2010) 737-742.
14. K.V.R. Murthy, B.N. Rao, B. N. Rajasekhar, B. Walter, R. Kumar, K.Suresh and B. S. Rao, *Physics Procedia* 29 (2012) 65–69.
15. Y. D. Jiang, F. Zhang, C. J. Summers and Z. L. Wang, *Appl. Phys. Lett.* 74 (1999) 1677-1679.
16. S. D. Bham, R. Prasad, *Int J Chemtech Res.* 9 (2016) 926-931.
17. M. Stefanski, D. Hreniak and W. Strek, *Optical Materials* 65 (2017) 95-98.
18. T. Xu, Q. Zhang, X. Yang, Q. Liu, L. Wang, Le Zhang and Q. Zhang, *J. Mater. Sci. Mater. Electron.* 28 (2017) 10131-10138.
19. Y. W. Seo, B. C. Choi, B. K. Moon, S. H. Park, J. H. Jeong, K. H. Kim and J. H. Kim, *Journal of Luminescence* 182 (2017) 240-245.

(2018) ; <http://www.jmaterenvirosci.com>